MDPI

Article

Equivalent Scheme of the Fuel Cell Taking into Account the Influence of Eddy Currents and A Practical Way to Determine Its Parameters

Alexander Pavlenko *, Yuri Burtsev, Ivan Vasyukov, Vladimir Puzin and Andrew Gummel

Energy Faculty, Platov South-Russian State Polytechnic University (NPI), Novocherkassk 346428, Russia
* Correspondence: eea.srspu@gmail.com; Tel.: +7-863-525-5113

Abstract: The aim of this work is to develop a dynamic equivalent scheme of the fuel cell, taking into account eddy currents in the conductive parts of the structure, to offer a practical way to determine the parameters of this circuit and also to show the adequacy of the scheme and parameters by numerical simulation and comparison with experiment. Fuel cells, as a rule, are connected to the voltage converters, which create a high-frequency component of the main fuel cell current and eddy currents in the conductive parts. The problem is that the effect of these currents on the characteristics of the fuel cell-based power plants has not been studied. To determine the parameters of the proposed equivalent scheme, we use experiments and calculations of transient modes of the fuel cell. The main result of the work is the possibility and feasibility of calculating circuits with fuel cells, taking into account the influence of eddy currents. This effect depends both on the design of the fuel cell and on the parameters of the circuit to which it is connected. From this it follows that, in general, it is necessary to take into account the influence of eddy currents of the fuel cell. The refusal of this accounting is possible, but in each specific case it must be justified.

Keywords: power plant; fuel cell; equivalent scheme; transient processes; modeling; experimental data; aerial vehicles

1. Introduction

One of the tasks related to the design and calculations of power plants based on fuel cells with proton exchange membranes (PEMFC) is the construction of an equivalent PEMFC scheme and the determination of its parameters. Different variants have been proposed to solve this problem. However, none of the methods known to us takes into account the influence of eddy currents that occur in metal electrodes and other conductive parts of the PEMFC structure due to the flow of the alternating high-frequency component of the current. This component inevitably arises due to the operation of semiconductor voltage converters, which, as a rule, are connected to the PEMFC. Thus, the problem consists in constructing an equivalent PEMFC scheme that takes into account eddy currents, and also in determining the parameters of this scheme.

The influence of eddy currents on the electrical processes in the PEMFC and the devices connected to it may be weak or significant, depending on the parameters of the circuit elements. At the same time, voltage and current overloads are possible, which is critically important to exclude at the stage of calculation and design of the product. Eddy currents dampen electrical oscillations and also lead to energy losses and heating. It is important to be able to calculate these phenomena at least to assess their significance in specific cases. If the influence of eddy currents is significant, then it should be taken into account and adjusted if necessary. In addition, the calculations of the PEMFC, taking into account eddy currents, are of theoretical scientific interest.

The development of an equivalent scheme of the PEMFC, taking into account the influence of eddy currents, seems to be a difficult task, primarily because it requires a

new look at the known and studied device. At the same time, it is important to correctly identify and take into account all significant physical factors. A separate task is the practical determination of the values of the parameters of an equivalent scheme. Solving this problem required ingenuity and original approaches to the experimental and computational part. In particular, it was necessary to consider transients occurring at different speeds.

The exact reason why this task was not solved earlier is unknown to us. It can be assumed that the presence of eddy currents did not attract the attention of researchers for the reason that the PEMFC is traditionally considered as a source of direct current. Moreover, the effect of eddy currents is not always noticeable in practice. Traditional equivalent schemes of a PEMFC usually consist of two or three resistors and only one capacitor (for example, [1]). Such schemes are suitable for calculating slow transients. Some known equivalent schemes also contain an inductor [2]. Such schemes can be used to simulate slow and fast processes, but they do not take into account energy losses caused by eddy currents in conducting elements. These losses in some modes can lead to a significant damping of electrical oscillations and the additional heating of the PEMFC.

A key component of our approach is to take into account the alternating high-frequency component of the current of the PEMFC. In particular, it takes into account the influence of eddy currents caused by this component. Another important feature is the use of fast–flowing and slow transients separately to determine the parameters of an equivalent PEMFC scheme. A key component of the results can be called the possibility of correct numerical modeling of processes in the PEMFC and associated circuits at the design stage. This makes it possible to avoid the electrical and thermal overloads of components and create a reliable product. The main results of the work are also the proposed new equivalent scheme of the PEMFC and the original practical method for determining parameters.

With the help of the numerical simulation of the PEMFC with a voltage converter connected to it and a load on the examples presented in the article, it is confirmed that with some combinations of circuit parameters, the action of eddy currents in the conductive structural elements can noticeably dampen oscillations, as well as increase energy losses and heat generation in the PEMFC. A comparison of the calculated and experimental data for the control experiment shows an excellent correspondence.

The new knowledge provided by the proposed article consists in the developed equivalent scheme of the PEMFC, which, in contrast to the known schemes, takes into account the influence of eddy currents in the conductive elements of the structure. The new results also include a practical experimental and computational method for determining the parameters of this scheme. This knowledge and these results are confirmed by examples of the numerical calculation of electrical circuits and fill the existing gap in the theory and methods of modeling of the PEMFC.

2. Equivalent Scheme

This research was initiated by the problem of creating a PEMFC-based power supply system for a small (1–2 kW power) unmanned aerial vehicle (UAV). Peak loads during maneuvers accompanied by changes of the fuel cell current are the specific feature of the operating modes of the UAV power plant. To solve this problem, special voltage stabilization circuits are used in the integration mode of the PEMFC stack and the battery [3–7]. In this case, a low-frequency part of the fuel cell alternating-current component, which is formed in transient modes when the load changes, is mostly compensated by battery connected in parallel with the load and with the help of a regulator that controls the voltage converter. The main high-frequency part of the fuel cell alternating-current component is caused by the operation of the voltage converter, although this fact is not found in the publications known [1,7–18].

It is possible to develop UAV electrical complex with the help of mathematical and computer modeling methods, to be more exact, by creating models of power plant subsystems, including the fuel cell to further combine them into a generalized computer model. This allows predicting the electrical complex parameters and characteristics at the design

stage, considering electrical processes in the fuel cell, and setting the requirements for control algorithms.

The voltage at PEMFC output significantly depends on the load current [8]. A fuel cell stack requires voltage and current stabilization in the range of about 70–110% of the nominal value. As mentioned above, such modes are provided by step-down transformerless converters [9–15] and batteries connected in parallel with the load and operating in a buffer mode. The converters consume current from PEMFC battery, containing DC and high-frequency pulse components. DC component generation is a regular function of the PEMFC. The influence of the alternating impulse current component on PEMFC operating modes has not yet been sufficiently studied. Therefore, these issues are raised in this paper.

The study of the alternating current effect on PEMFC implies two aspects. The first is the study of possible changes in chemical reactions under the alternating current. This task falls within the electrochemistry field. The second is the study of PEMFC response to alternating current as an electrical circuit element. This task may be attributed to the competence of theoretical and applied electrical engineering.

Another important design task is the calculation of overloads of circuit elements by voltage and current. It is recommended to solve this problem for the entire system, as its processes differ significantly in characteristic frequencies and time constants. In this case, the synchronization of peak loads from different frequencies may cause a critical overload. The system is complicated, so ordinary engineering intuition and experience may not be sufficient to create a reliable operating device. It is easier and cheaper to perform the required tests first on a numerical model and then on a full-scale specimen.

Most of the known equivalent schemes consist of resistors and capacitor (Figure 1). Such circuits might be used only to model low-frequency (less than 1 Hz) periodical processes or transient processes with big (more than 1 s) time constants because capacitance C is very high (several farads). Real PEMFC work with high (10 kHz and above) frequencies.
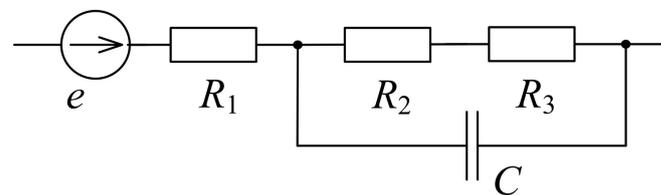

Figure 1. Traditional active-capacitive fuel cells with proton exchange membranes (PEMFC) dynamic equivalent scheme. Here e is electromotive force of the fuel cell; R_1, R_2 and R_3 are resistors, C is a capacitor.

Some existing equivalent schemes contain an inductor (Figure 2). This makes it possible to model high frequency periodical processes and fast transient processes. On the other hand, such schemes do not take into account power losses caused by eddy currents in metal plates and other conductive elements. If there is alternating and especially high frequency current in conductors, it initiates eddy currents caused by the time variation of magnet field created by primary current. The influence of these eddy currents may be significant in some cases and should not be neglected.
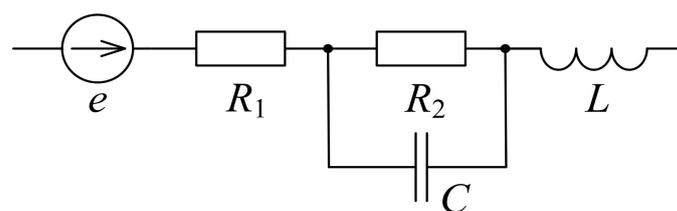

Figure 2. Traditional fuel cells with proton exchange membranes (PEMFC) dynamic equivalent scheme with inductor. Here e is electromotive force of the fuel cell; R_1 and R_2 are resistors, C is a capacitor, L is inductor.

The authors propose an option of the fuel cell dynamic equivalent scheme, shown in Figure 3. Electromotive force e is the equivalent fuel cell EMF; C is the capacity generated by the electrochemical effect of double layer of electric charges at the interface between electrodes and the proton-conducting membrane; L is the parasitic inductance of PEMFC circuit; R_1 is active internal resistance of the PEMFC caused by specific ohmic resistance of the conductors; R_2 is resistance simulating the energy losses due to polarization activation inside PEMFC; R_3 is active dynamic resistance for modelling energy losses from eddy currents in metal electrode plates and other conductors; and R_4 is the load resistance.
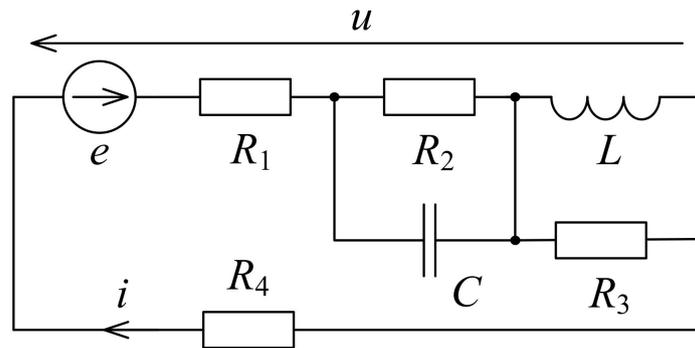

Figure 3. The fuel cells with proton exchange membranes (PEMFC) dynamic equivalent scheme taking into account eddy currents in the conductors. Here e is electromotive force of the fuel cell; $R_1 - R_3$ are resistors, C is a capacitor, L is inductor of the PEMFC equivalent scheme; R_4 is load resistor; u is voltage an i is current of the PEMFC.

The scheme with dynamic losses effect reflects the physical reality; resistor R_3 with parallel inductance does not prevent flow of current i steady component, but it dampens the alternating component of this current. Eddy currents arise due to magnetic field variations generated by the main current. The equivalent scheme parameters are determined by experimental data. The difference of this circuit in comparison to the more widely used types [1,2,16–18] mainly consists in the influence of dynamic losses in conductors. Obviously, this influence is present and might be quite significant if caused by rapidly changing large currents. However, the authors are not aware of any papers which consider or mention such an issue. Eddy currents dampen electrical oscillations in the PEMFC circuit, absorbing energy and causing heating. In some operating modes with certain parameters of the power plant, their influence can be negligible, but it can be of importance in other modes and with other parameters.

3. Equivalent Scheme Parameters Evaluation

The PEMFC equivalent scheme parameters might be determined as follows. Electromotive force e and the sum of resistances $R_1 + R_2$ can be obtained from the solution of the system of equations according to the results of two experiments on PEMFC stack loading with direct current within approximate linearity of the V-I characteristic (Equation (1)):

$$\begin{cases} e - i_1(R_1 + R_2) = u_1 \\ e - i_2(R_1 + R_2) = u_2 \end{cases}, \tag{1}$$

where u_1, u_2 are PEMFC voltages, and i_1, i_2 are corresponding currents at different loads R_{41} and R_{42}. When loaded with direct current, inductance L, resistor R_3, and capacitor C are excluded from the circuit (Figure 4). It makes no practical sense to model PEMFC either at very low or very high currents in the non-linear sections of its V-I characteristic since the PEMFC does not operate in such modes. In the analyzed experiments, PEMFC is loaded directly with the R_4 resistor without voltage converter. To improve the accuracy and reduce the influence of random errors, instead of solving system (1), one can determine the same parameters e and $R_1 + R_2$ from several points of experimental V-I characteristic

of PEMFC stack by the least squares method. For PEMFC prototype, with 1/4 of the working fuel cell installed on the experimental UAV, the following values are obtained: $u_1 = 20.0$ V; $u_2 = 14.8$ V; $i_1 = 2.0$ A; and $i_2 = 16.0$ A. The parameters $e = 20.743$ V and $R_{12} = R_1 + R_2 = 0.371$ Ohm are calculated based on the mentioned values.
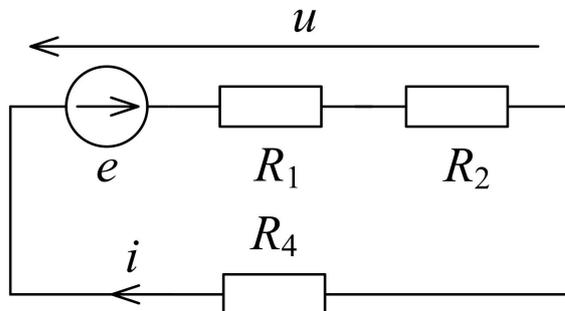

Figure 4. The fuel cells with proton exchange membranes (PEMFC) equivalent scheme for the DC current component. Here e is electromotive force of the fuel cell; R_1 and R_2 are resistors of the PEMFC equivalent scheme; R_4 is load resistor; u is voltage an i is current of the PEMFC.

For further studies, we use stiffness of the equation system to describe transients in the dynamic equivalent scheme shown in Figure 3. Experimental data and calculated estimates show that the duration of transient associated with the inductance L is about three orders of magnitude shorter than the duration of process with capacitance C. It makes it possible to study these processes separately. We will change the load resistance abruptly from high value $R_{41} = 10$ Ohm to low value $R_{42} = 0.938$ Ohm (load rise). The same resistances were used to determine PEMFC static parameters.

It is necessary to consider the state of the circuit right after the end of the fast transient associated with inductance. During this time, the voltage across the capacitor cannot significantly change its value, resistor R_3 will be practically shunted by inductance L as the transient process with the inductance is completed. Therefore, the jump of the load voltage (Figure 5) is related to the changing current in the resistor R_1 (Equation (2)):

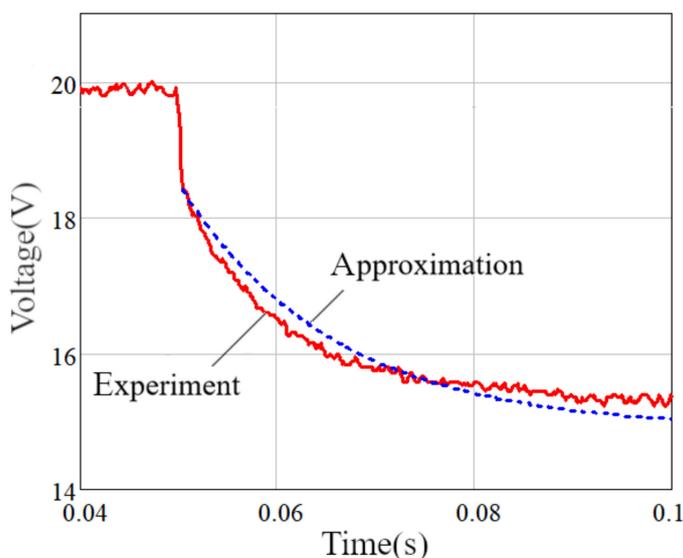$$\Delta u = R_1 \cdot (i(+0) - i(-0)) \tag{2}$$

Figure 5. Surge of the fuel cells with proton exchange membranes (PEMFC) and load voltage when load resistance decreases (load rise). Experiment and approximation.

By the current limiting value on the right, we get its value immediately after the end of the transient process with inductance.

In the experiment with the resistive load rising, a voltage surge $\Delta u = 1.3$ V was got with current limiting values of $i(-0) = 2.0$ A; $i(+0) = 20.0$ A. At load shedding, respectively, $\Delta u = 1.0$ V; $i(-0) = 16.0$ A; $i(+0) = 2.0$ A. Calculated resistance values R_1 are, respectively, equal to 0.072 Ohm and 0.071 Ohm. For further calculations, $R_1 = 0.071$ Ohm. As $R_{12} = R_1 + R_2 = 0.371$ Ohm, we determine $R_2 = 0.3$ Ohm. For voltage change curves, we define approximations by calculating the time constants by solving non-linear equations $S = 0$ using the dichotomy method, where S is the average deviation of the approximation from the experimental data in the active phase of the transient process. For load rising, we obtain the function (Equation (3))

$$u(t) = 14.9 + 3.6 \exp((t - t_0)/0.015) \text{ (V)}, \tag{3}$$

for shedding (Equation (4))

$$u(t) = 20 - 4 \exp((t - t_0)/0.021) \text{ (V)}. \tag{4}$$

It is clear that the time constant for the circuit shown in Figure 3, without inductance L and resistor R_3, is equal to $\tau = C \cdot R_2 \cdot (R_1 + R_4) \div (R_1 + R_4 + R_2)$. By substituting the corresponding values of τ and resistances into this equation, it is possible to determine the capacitance C. When the load rises, it is 0.0668 F, when the load sheds, it is 0.0734 F. For further calculations, we take the average value of $C = 0.0701$ F. The experimental and calculated time dependences of PEMFC voltage and current are demonstrated in Figure 6.
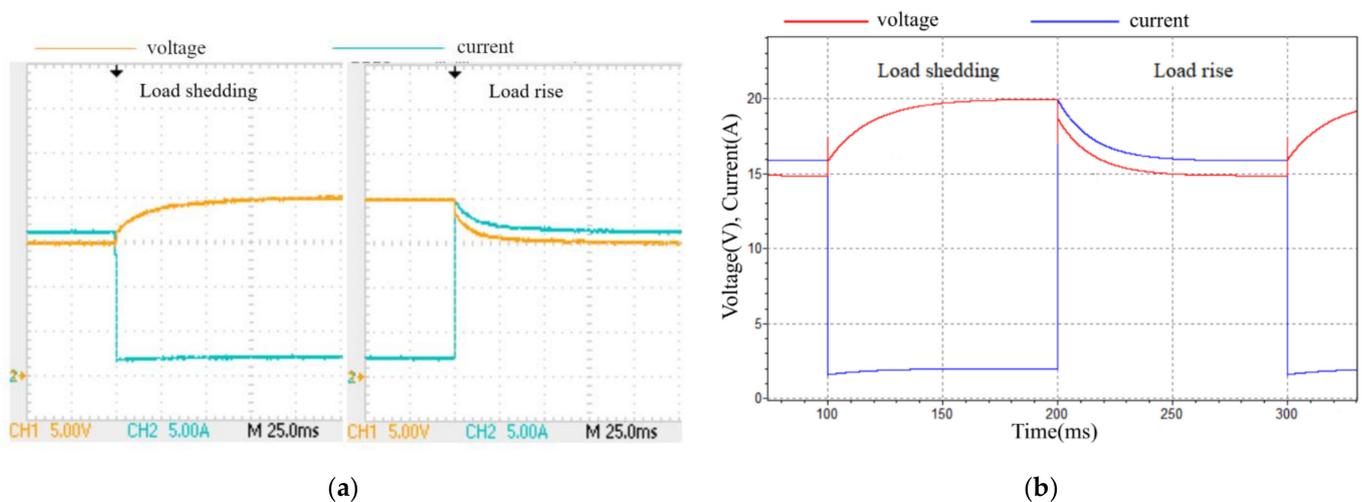

Figure 6. Experimental (**a**) and calculated (**b**) fuel cells with proton exchange membranes (PEMFC) voltage and current for load shedding and rise.

The calculations were performed with the "Electroscope" program, created by the authors of this paper. Its description is presented in [19]. The program is characterized by an increased reliability in calculations of circuits with commutations.

In the equivalent scheme, it is also necessary to determine inductance L and resistance R_3. The experimental design to determine these parameters is shown in Figure 7.

An additional test capacitor C_0 has much lower capacity than the capacitor C. This is why during the transient process of the capacitor C_0 charging, voltage across the capacitor C changes insignificantly. Practically, it works as a voltage source, and the equivalent scheme for the free component of this transient process is as shown in Figure 8.
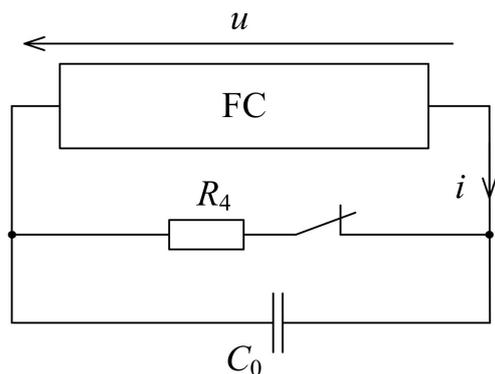
Figure 7. The experimental design to determine inductance L and resistance R_3. FC for fuel cell. Here FC is the fuel cell, R_4 is load resistor, C_0 is an external capacitor, u is voltage an i is current of the fuel cell.
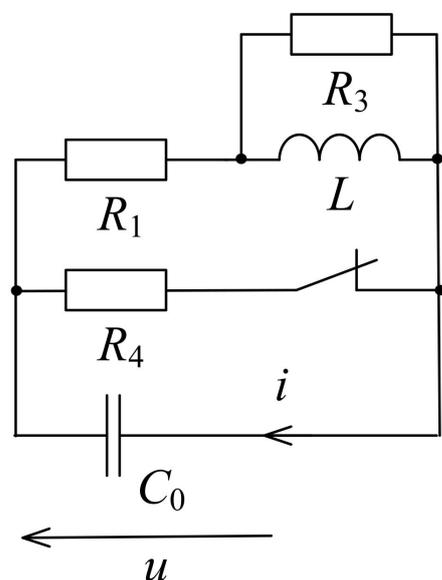

Figure 8. The equivalent scheme for the free component of the transient with inductance. Here R_1 and R_3 are resistors and L is inductance of the fuel cell equivalent scheme, R_4 is load resistor, C_0 is an external capacitor, u is voltage an i is current of the fuel cell.

After opening the key, resistor R_4 is excluded from the circuit. The capacitor $C_0 = 1.768$ μF is selected so that the transient process is oscillatory. The characteristic equation for the resulting circuit is as follows: $(R_1 + R_3) \cdot L \cdot C_0 \cdot p^2 + (R_1 \cdot R_3 \cdot C_0 + L)p + R_3 = 0$.

The equation solution can be represented as $p_1 = -\delta + j\omega$, $p_1 = -\delta - j\omega$, where

$$\delta = (R_1 R_3 C_0 + L)/2LC_0(R_1 + R_3), \tag{5}$$

$$\omega = \frac{\sqrt{4(R_1 + R_3)R_3 LC_0 - (R_1 R_3 C_0 + L)^2}}{2(R_1 + R_3)LC_0} \tag{6}$$

These equations can be converted to two linear equations for L and R_3. As result of solving the equations, these two parameters are determined if all the others are known:

$$\alpha = (\delta^2 + \omega^2)/((2\delta - (\delta^2 + \omega^2)R_1 C_0)), \ L = (\alpha - (\delta^2 + \omega^2)R_1 C_0)/\alpha(\delta^2 + \omega^2)C_0, \ R_3 = \alpha L. \tag{7}$$

The values of δ and ω can be determined from the digital oscillogram using any optimization method because the solution of the problem does not depend on the used solving method. The target function can be norm of the difference between the experimental data and the approximation of the form $u(t) = A\exp(-\delta(t - t_0))\cos(\omega(t - t_0))$. Resistance to

and the reactance of the conductor with alternating currents depend on the frequency [20], which, apparently, can be observed on the oscillogram. The time dependence of circuit parameters can be taken into account by constructing a more complex active-inductive equivalent scheme, but in terms of this paper we refer to the first approximation in the form of one inductance L and one resistor R_3. For more complicated equivalent schemes, it is not yet possible to obtain circuit parameters using simple formulae.

　　　The experimental oscillogram of the voltage across the capacitor C_0 when load the R_4 switches off and its approximation are shown in Figure 9. From this oscillogram that was taken from the oscilloscope in digital form, in accordance with the coordinate descent method, values $\delta = 6.724 \times 10^4$ 1/s and $\omega = 6.774 \times 10^5$ rad/s are calculated, the time interval varies from 101.6 to 150 μs. However, due to the fact that the frequency and attenuation coefficient of the experimental data change during the transient process, these values need to be specified. To improve approximation accuracy, they are corrected according to the graph. As a result, the approximate values of transient process parameters $\delta = 5.263 \times 10^4$ 1/s and $\omega = 6.68 \times 10^5$ rad/s are obtained. According to the formulae above, the circuit parameters are as follows: $L = 1.252$ μH and $R_3 = 12.737$ Ohm. The calculations consider the equivalent series resistance of the capacitor (ESR) 6 mOhm. This resistance ESR, as well as equivalent resistance R_1, has a noticeable effect on the parameter values.
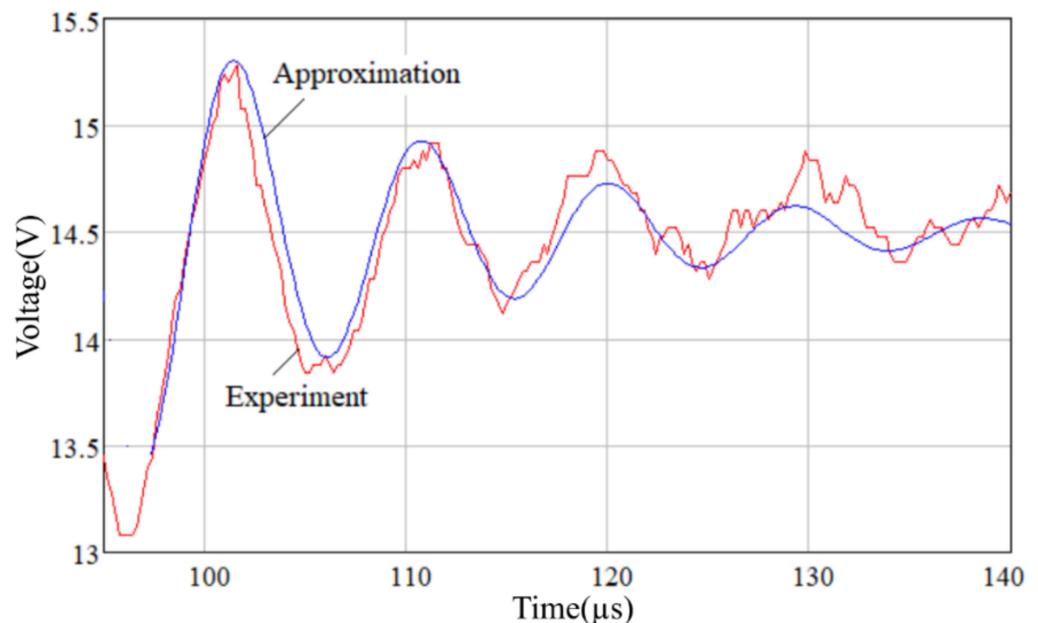

Figure 9. Voltage across the capacitor C_0, experiment and approximation.

　　　Using the known parameters of the PEMFC equivalent scheme, it is possible to calculate the options for power plant operating modes, select the parameters of its elements that provide the specified energy indicators. The calculation of the voltage and current overloads of semiconductor elements is critically important; this calculation is impossible without an adequate equivalent scheme for PEMFC in transient modes. In this case, it is important to consider circuit inductance and oscillation damping. Without full consideration of these factors, numerical modeling results may differ from the real device processes.

　　　To illustrate the PEMFC model features, let us consider the power plant electrical complex based on PEMFC, shown in Figure 10. One of the design stage tasks is to determine the capacitance of capacitor C_7, connected in parallel to the PEMFC to quench overvoltages on the semiconductor switches. These overvoltages arise due to the interruption of currents in the two-wire line connecting PEMFC and voltage converter. Since this line and the PEMFC itself have parasitic inductances and the rate of current change is very high, in the absence of a capacitor, overvoltages result in additional thermal losses in the keys and the possible electrical breakdown of semiconductor devices. A justified choice of the

capacitance C_7 is possible only by using numerical modeling. Figures 11–14 present the calculated oscillograms showing the effect of the capacitance C_7 and the active-inductive part of equivalent scheme on PEMFC operation with 1250 W resistive load. Figure 15 shows voltage and current of the PEMFC with converter and 224 W resistive load, simulation, and experimental results. Calculations are performed in the "Electroscope" program.
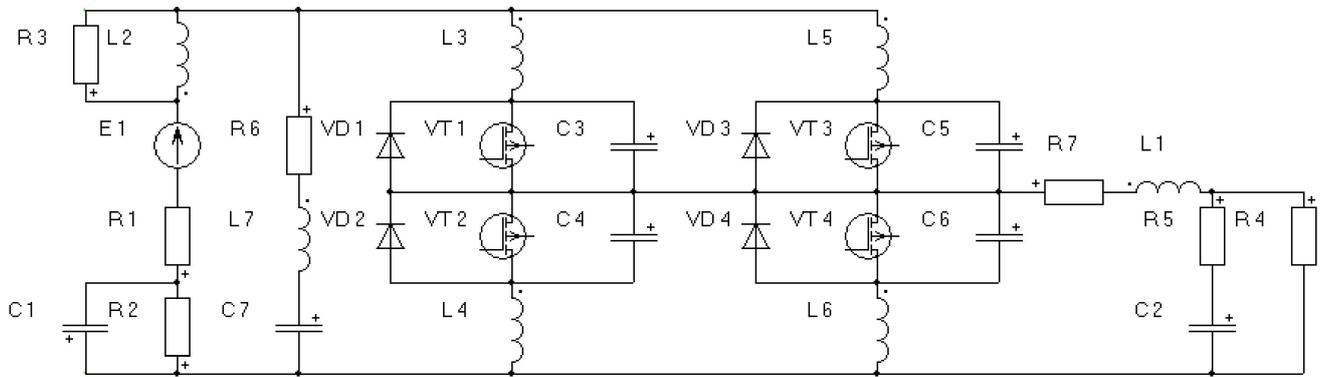

Figure 10. Scheme for numerical modeling of fuel cells with proton exchange membranes (PEMFC) based power plant. Here E_1, R_1, R_2, R_3, C_1, and L_2 are PEMFC equivalent scheme elements. Resistors R_5-R_7, inductances L_3-L_7 and capacitors C_3-C_6 are small parasitic parameters, C_2 and C_7 are external capacitors, L_1 is external inductor and R_4 is load resistor. "Electroscope" program screenshot.
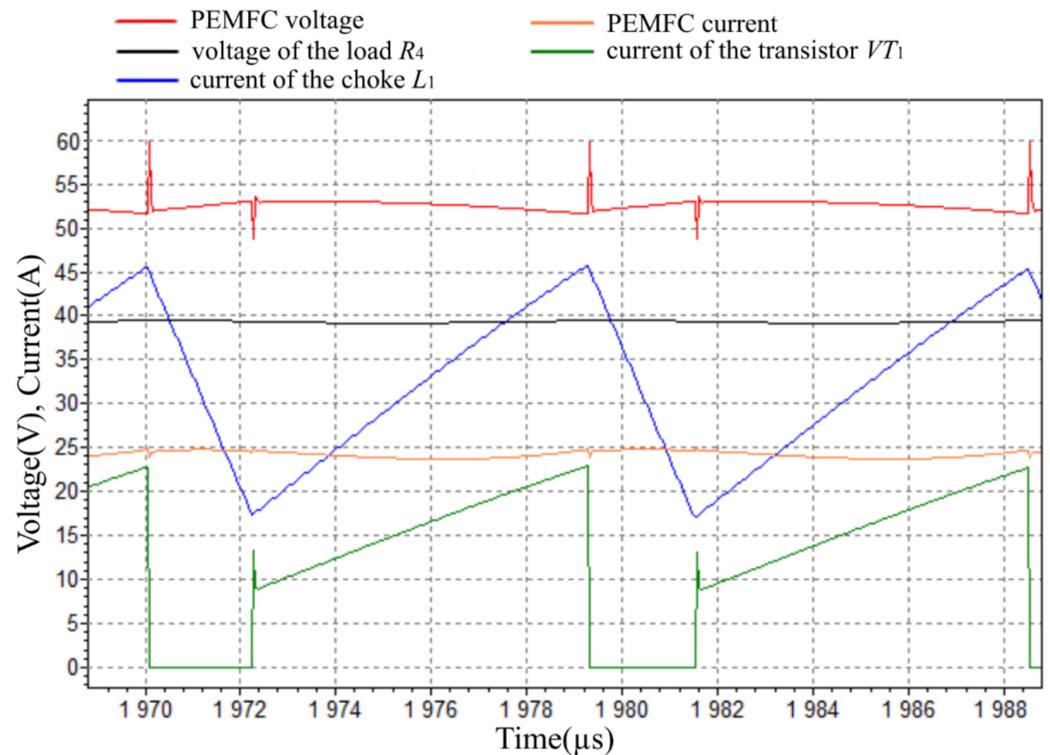

Figure 11. Simulation oscillogram. Capacity, $C_7 = 47$ μF; resistance, $R_3 = 12.737$ Ohm. Normal operating mode of experimental fuel cells with proton exchange membranes (PEMFC) based power plant. That correspond to the proposed equivalent scheme (Figure 3). RMS voltage of the resistor R_3 is 0.646 V, power is 33 mW. The results are very close to real experimental data.
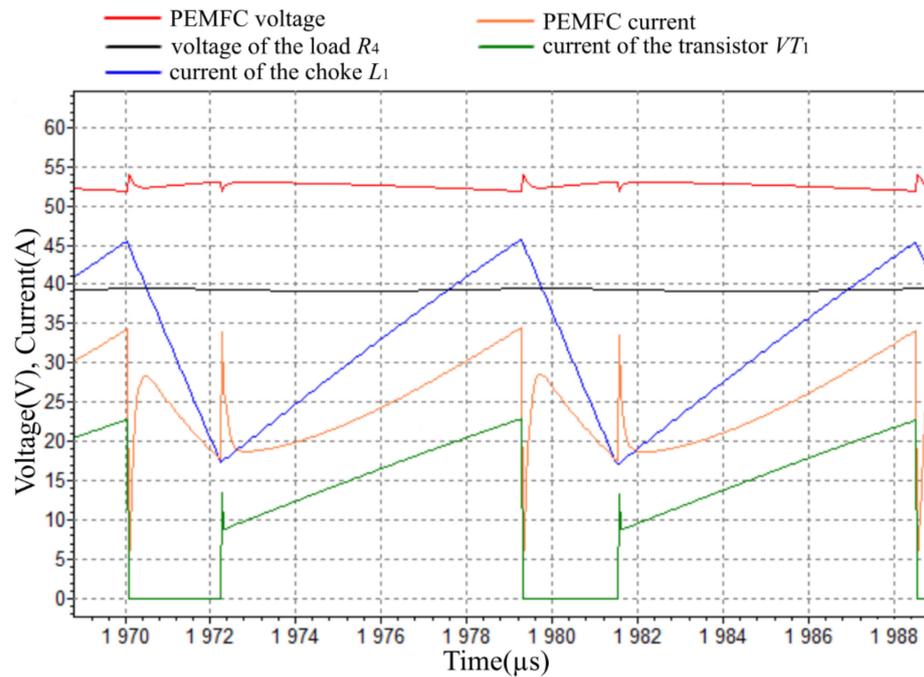
Figure 12. Simulation oscillogram. Capacitor, $C_7 = 47$ μF, and resistance, R_3, was intentionally set to zero, the active-inductive part of the fuel cells with proton exchange membranes (PEMFC) equivalent scheme is absent. This correspond to the traditional active-capacitive equivalent scheme (Figure 1). The incorrect calculation of the PEMFC current.
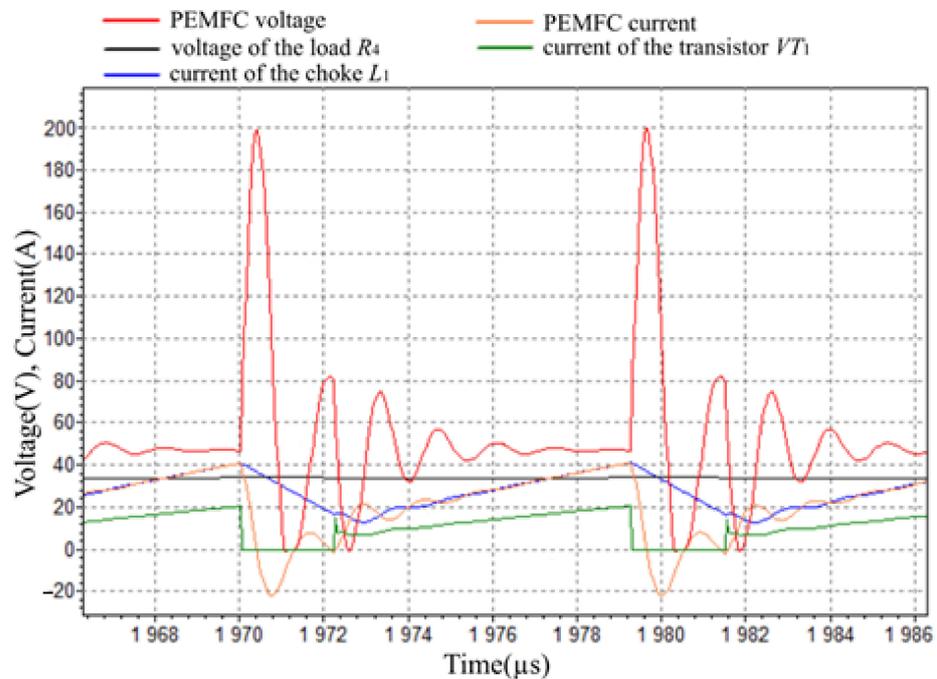

Figure 13. Simulation oscillogram. Capacitor $C_7 = 47$ nF is too small. Abnormal operating mode. Resistance $R_3 = 12.737$ Ohm has the value calculated according experiments. This corresponds to the proposed equivalent scheme (Figure 3). The noticeable damping of the fuel cells with proton exchange membranes (PEMFC) voltage and current oscillations. The RMS voltage of the resistor R_3 is 36.08 V and the power is 102.2 W.
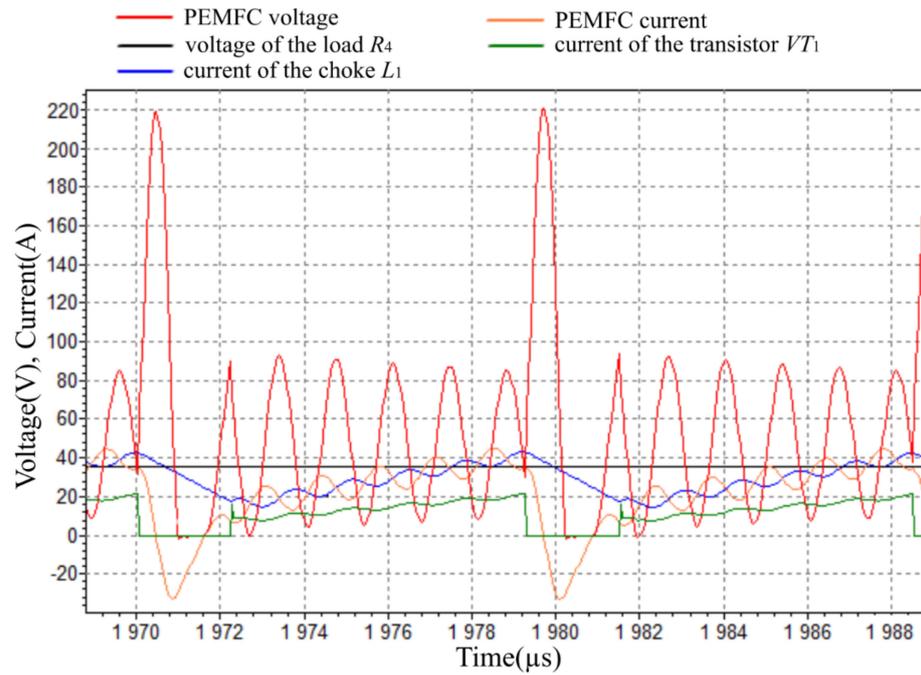
Figure 14. Simulation oscillogram. Capacitor C_7 = 47 nF is too small. Abnormal operating mode. An intentional circuit break instead of resistance R_3. This corresponds to the traditional equivalent scheme with inductor (Figure 2). Mistakenly weak damping of the fuel cells with proton exchange membranes (PEMFC) voltage and current oscillations.
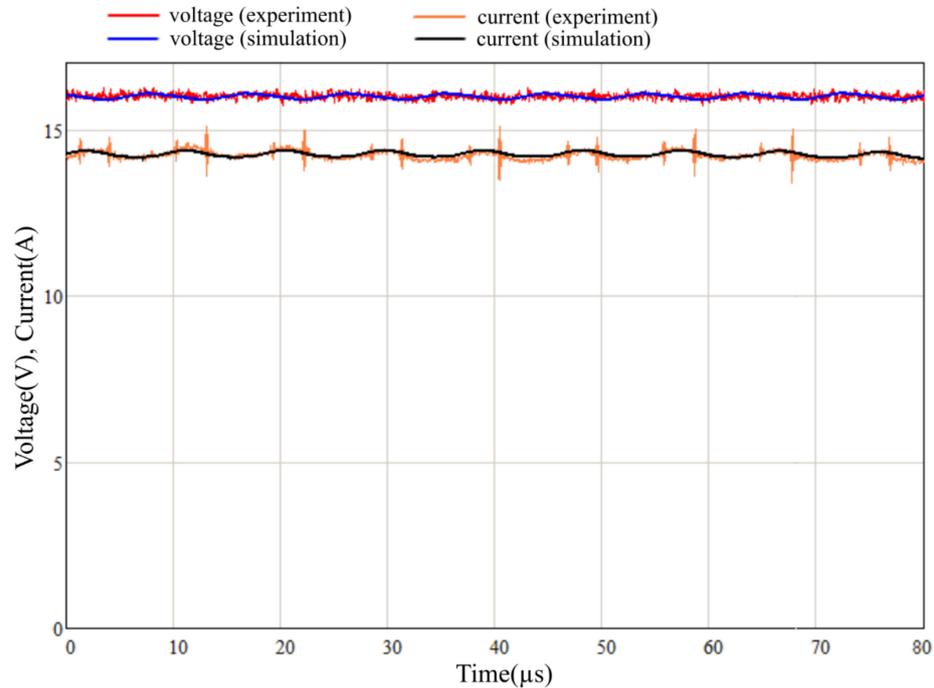

Figure 15. Voltage and current of the real fuel cells with proton exchange membranes (PEMFC) with converter and 224 W resistive load, C_7 = 250 μF. The proposed equivalent scheme of the fuel cell. Comparison of the experiment and simulation shows insignificant difference that is caused mostly by high frequency interferences in measuring circuits.

4. Results and Discussion

The first result of the presented research is a new model of PEMFC, which, in addition to the phenomena traditionally taken into account, takes into account eddy currents in metal electrodes and other conductive structural elements. Taking into account eddy currents seems natural and necessary, since they are necessarily induced in any conducting bodies in the presence of an alternating electromagnetic field. In the case of PEMFC, eddy currents are excited by the high-frequency component of the current, which arises as a result of the operation of voltage converters commonly used together with PEMFC.

The fact that up to now the calculations of circuits with PEMFC have been carried out without taking into account eddy currents suggests that in many practical cases the effect of these currents is weak. However, as the comparison of Figures 13 and 14 shows, for example, in some cases the influence of eddy currents can be noticeable. At least, the refusal to take into account this influence in the general case should be justified, since this phenomenon itself always takes place. Taking into account eddy currents makes the equivalent scheme of the PEMFC more accurate and correct. This leads to more adequate calculations at the product design stage and increased reliability.

The second result is an original method of practical experimental and computational determination of the values of the parameters of the proposed equivalent scheme. It allows the parameter values for circuit elements by several simple experiments and calculations to be obtained. Without this technique, the value of the scheme would not be so big. It is essential that the new equivalent scheme does not require any special laboratory equipment and complex calculations for its use. That is, the improvement of the design quality is achieved without additional costs.

The third result is the presented numerical calculations of the operating modes of the PEMFC together with the voltage converter. They show the way to use the equivalent scheme of the PEMFC, make it possible to compare operating modes with different circuit parameters. In particular, these calculations show that in some cases the action of eddy currents can be noticeable and may deserve attention. Numerical calculations also show excellent accordance with the data obtained experimentally on a real PEMFC (Figure 15). This proves the correctness of the approaches and assessments made in the work.

5. Conclusions

The article proposes a dynamic equivalent scheme for the PEMFC, which, unlike the known schemes, takes into account eddy currents in metal plates of electrodes and other conductors. These currents affect the transients in the PEMFC circuit and the PEMFC itself. Without full consideration of this factor, the results of numerical simulation may differ from the actual processes in the device. In the studies known to us, eddy currents are not taken into account.

An original method of the experimental investigation of the PEMFC and the subsequent calculation of the parameters of the developed equivalent scheme for the PEMFC based on the results of the experiment is proposed. A study of transients in the electrical part of a power plant based on the PEMFC, taking into account the parameters of the fuel cell block, was carried out. Unlike most of the relevant studies, switchings in a step-down voltage converter are considered as the source of these processes corresponding to the actual operating conditions of the power plant. The calculations performed make it possible to determine the parameters of the power plant at the design stage and with the help of computational experiments to study the operation of the installation in various modes. The results of the numerical simulation of the power plant based on the PEMFC show an excellent correlation with experimental data.

For further work on the topic of the article, the following considerations can be considered. First, we can try to do the experiment with oscillatory transient process for determining the inductance L and resistance R_3 in another way, so that the amplitude of voltage oscillations is greater.

This will reduce extraneous influences and measurement errors. This can be carried out by connecting the PEMFC to the capacitor. Before the connection, the PEMFC can be in idle mode or in normal load mode and the capacitor can be discharged or charged to some reverse polarity voltage. Secondly, numerical experiments are of interest, which would make it possible to more accurately determine the conditions under which the influence of eddy currents is noticeably manifested.

Author Contributions: Conceptualization, A.P. and Y.B.; methodology, I.V.; software, A.G.; validation, Y.B., I.V. and A.G.; formal analysis, V.P.; investigation, Y.B.; resources, V.P.; data curation, A.P.; writing—original draft preparation, Y.B.; writing—review and editing, A.P.; visualization, I.V.; project administration, A.P.; funding acquisition, V.P. All authors have read and agreed to the published version of the manuscript.

Conflicts of Interest: The authors declare no conflict of interest.

References

1. Outeiro, M.T.; Chibante, R.; Carvalho, A.S.; de Almeida, A.T. Dynamic modeling and simulation of an optimized proton exchange membrane fuel cell system. In *ASME International Mechanical Engineering Congress and Exposition*; IMECE2007-43558; ASME: Seattle, WA, USA, 2007; pp. 171–178. [CrossRef]
2. Narjiss, A.; Depernet, D.; Gustin, F.; Hissel, D.; Berthon, A. Design of a High Efficiency Fuel Cell dc/dc Converter Dedicated to Transportation Application. *J. Fuel Cell Sci. Technol.* **2008**, *5*, 041004. [CrossRef]
3. Savvaris, A.; Xie, Y.; Malandrakis, K.; Lopez, M.; Tsourdos, A. Development of a Fuel Cell Hybrid-Powered Unmanned Aerial Vehicle. In Proceedings of the 2016 24th Mediterranean Conference on Control and Automation (MED), Athens, Greece, 21–24 June 2016. [CrossRef]
4. Oheda, H. *Artificial Neural Network Control Strategies for Fuel Cell Hybrid System*; Cranfield University: Bedford, UK, 2013.
5. Karunarathne, L. *An Intelligent Power Management System for Unmanned Aerial Vehicle Propulsion Applications*; Cranfield University: Bedford, UK, 2012.
6. Virji, M. *A Novel Proton Exchange Membrane Fuel Cell-Battery Partial Hybrid System Design for Unmanned Aerial Vehicle Application. Knowledge Foundation's 14th Annual International Symposium*; Hawaii Natural Energy Institute: Honolulu, HI, USA, 2012.
7. Strele, T. Power Management for Fuel Cell and Battery Hybrid Unmanned Aerial Vehicle Applications. Master's Thesis, Arizona State University, Tempe, AZ, USA, 2016.
8. Hoogers, G. *Fuel Cell Technology Handbook*, 1st ed.; CRC Press: Boca Raton, FL, USA, 2002. [CrossRef]
9. Kolli, A.; Gaillard, A.; De Bernardinis, A.; Bethoux, O.; Hissel, D.; Khatir, Z. A review on DCDC converter architectures for power fuel cell applications. *Energy Convers. Manag.* **2015**, *105*, 716–730. [CrossRef]
10. Gao, D.; Jin, Z.; Liu, J.; Ouyang, M. An interleaved step-up/step-down converter for fuel cell vehicle applications. *Int. J. Hydrog. Energy* **2016**, *41*, 22422–22432. [CrossRef]
11. Gao, D.; Jin, Z.; Zhang, J.; Li, J.; Ouyang, M. Development and performance analysis of a hybrid fuel cell/battery bus with an axle integrated electric motor drive system. *Int. J. Hydrog. Energy* **2016**, *41*, 1161–1169. [CrossRef]
12. Tao, L.E.; Zhou, Y.A.; Zicun, L.I.; Zhang, X. State of art on energy management strategy for hybrid-powered unmanned aerial vehicle. *Chin. J. Aeronaut.* **2019**, *32*, 1488–1503. [CrossRef]
13. Kabalo, M.; Paire, D.; Blunier, B.; Bouquain, D.; Godoy Simões, M.; Miraoui, A. Experimental evaluation of four-phase floating interleaved boost converter design and control for fuel cell applications. *IET Power Electron.* **2013**, *6*, 215–226. [CrossRef]
14. Harfman Todorovic, M.; Palma, L.; Enjeti, P.N. Design of a Wide Input Range DC–DC Converter With a Robust Power Control Scheme Suitable for Fuel Cell Power Conversion. *IEEE Trans. Ind. Electron.* **2008**, *55*, 1247–1255. [CrossRef]
15. Fardoun, A.A.; Ismail, E.H.; Sabzali, A.J.; Al-Saffar, M.A. Bidirectional converter for high-efficiency fuel cell powertrain. *J. Power Sources* **2014**, *249*, 470–482. [CrossRef]
16. Xu, L.; Xiao, J. Modeling and Simulation of PEM Fuel Cells Based on Electrochemical model. In Proceedings of the 2011 International Conference on Remote Sensing, Environment and Transportation Engineering, Nanjing, China, 24–26 June 2011. [CrossRef]
17. Arsov, G.L. Improved Parametric PSpice Model of a PEM Fuel Cell. In Proceedings of the 11th International Conference on Optimization of Electrical and Electronic Equipment, Brasov, Romania, 22–24 May 2008. [CrossRef]

18. Dachuan, Y.; Yuvarajan, S. Electronic circuit model for proton exchange membrane fuel cells. *J. Power Sources* **2005**, *142*, 238–242. [CrossRef]
19. Burtsev, Y.A.; Pavlenko, A.V.; Vasyukov, I.V. Calculation of transient modes in semiconductor converters using static resistances and the implicit Euler method. *Electr. Eng.* **2020**, 13–19. [CrossRef]
20. Neiman, L.R.; Demirchyan, K.S. *Theoretical Foundations of Electrical Engineering*; Energiya: Moscow/Leningrad, Russia, 1966. (In Russian)